RSC Advances

PAPER

View Article Online
View Journal | View Issue

Cite this: *RSC Adv.*, 2022, **12**, 22402

Preparation of coated paper reinforced by a blend of anionic-starch-based nanocellulose/chitosan and its properties

Meigui Xue, *[a] Zhou Wen,[a] Ruquan Huang,[a] Xinsheng Chai, [bc] Wei Li,[a] Chunxia Chen[c] and Hongqian Chen[d]

Carboxylated cellulose nanocrystal whisker (C-CNC) and chitosan (CTS) were used to blend and reinforce anionic starch (AS) to prepare a paper-coating agent, AS-CNC-CTS, which was coated on one side of the surface of offset paper and kraft paper. Scanning electron microscopy (SEM) showed that the AS-CNC-CTS coating agent can form a layer of dense film on the paper surface and fill the surface pores. And also, owing to the irregular pore structure of the paper, the coating agent penetrated the pores to different degrees. The structure and mechanical properties of the coated paper were analyzed using a Fourier infrared spectrometer, computer-controlled paper-tearing tester and paper tensile strength test machine. Peptide bonding interaction between C-CNC and CTS, hydrogen bonding between C-CNC and CTS, C-CNC and AS, C-CNC and paper fibers, as well as electrostatic attraction between acidified CTS and AS were found. Moreover, the coating agent also had good antibacterial properties, and no mold spots formed throughout the observation period (60d). The gas-barrier properties and oil resistance of the coated paper were further studied using a paper and paperboard air permeability tester and a paper oil-permeability tester. Results showed that the coating agent can significantly enhance the gas-barrier properties and oil resistance of paper. Furthermore, with increased C-CNC content in the coating agent, its barrier properties gradually increased. This finding indicated that the coating preparation had no effect on the crystal region of C-CNC.

Received 27th June 2022
Accepted 27th July 2022

DOI: 10.1039/d2ra03955a

rsc.li/rsc-advances

1 Introduction

Plastics are used in considerable proportions in the packaging industry for the excellent properties of plasticity, barrier property, toughness, and high strength.[1] The global demand for plastics increased at an average annual rate of 3.9% from 2015 to 2018, and is predicted to account for 20% of the total oil consumption by 2050.[2–4] However, plastic materials can cause great pressure on the environment due to the non-degradability. Meanwhile the toxic and harmful small-molecule substances in the plastic materials can migrate into packaged food when the plastic is to be a food contacting material. Therefore, many studies are exploring which materials can replace plastic packaging materials for food.[5–7] Owing to the abundant sources of raw materials, environment friendliness, good printability, and other properties, the amount of paper used in packaging is second only to plastic, so paper is very likely to replace plastic in packaging. However, paper has a porous structure formed by interwoven fibers. The porosity of uncoated paper has been analyzed using the threshold regression method in the early stage, and results showed that the porosity of uncoated paper accounts for 40–55%.[8] Owing to this structural basis, the smoothness, glossiness, and barrier property of paper materials are poor. Thus, the modification of paper-based materials to make it degradable and meet the requirements of mechanical and barrier properties required by packaging has become a research hotspot.[9–12]

Many methods have been used to modify paper-based materials.[13–16] Among them, the dip coating of oil, paraffin, resin, latex, *etc.*, to deposit a dense oxide film on the paper surface and laminate plastic on paper surface are extensively used and effective methods. However, most materials modified by the above-mentioned methods do not degrade naturally, so recycling waste paper is difficult and the energy consumption during the production increases. Therefore, under the background of the ban on plastic, carbon emission peak, and carbon neutrality, the surface-coating method with relatively simple process and easy production is the main method of studying paper modification at present. Meanwhile, in practice, to prevent mildew generation on paper materials when the environmental humidity reaches more than 80%, adding a desiccant and mildew-proof sheet in the processing of paper

[a]*Dongguan Polytechnic, Dongguan 523808, China. E-mail: meigui837616@163.com; Tel: +86-13669881074*
[b]*South China University of Technology, Guangzhou 510641, China*
[c]*Dongguan Quality of Testing, Dongguan 523808, China*
[d]*Beijing Technology and Business University, Beijing 100048, China*

packaging containers (such as cartons, paper bags, boxes, *etc.*) is usually necessary, however, it leads to the complexity of process and also lower the production efficiency. So food packaging materials should have good barrier performance against gas, oil as well as bacteria to protect the packaged food from various contamination, such as migratable hydrocarbons in paper and Gram-positive bacteria, *Staphylococcus aureus*, *etc.*, then prolong the food preservation and shelf life.[17–20] Therefore, the preparation of surface-coating agents for paper-based food packaging materials to exert a barrier effect and inhibit bacteria is the main content of this paper.

As a renewable resource with rich reserves and good degradation performance in nature, starch has become a common coating and sizing agent for paper modification owing to its good viscosity and film-forming property. It can effectively improve the surface gloss and smoothness of paper,[21] however, the mechanical property and barrier property of formed film are poor owing to its semicrystal properties.[22] Nanocellulose is a new bio-based polymer functional material developed in recent years. It is characterized by large specific surface area, renewability, good biocompatibility, low density, high strength, biodegradability, and wide source of raw materials, so it is extensively used in different paper-based functional materials and also has potential application value in reinforcement and barrier design.[6,7,23–25] Chitosan (CTS) is a natural amino polysaccharide with good antibacterial activity, film-forming property, and biodegradability. Its application and research in the fields of food packaging, fruit and vegetable preservation are attracting increased attention. However, CTS film has some disadvantages, such as weak mechanical properties.[26,27]

While there is no study on the components of anionic-starch-based nanocellulose/chitosan, and also the application of it. So in this paper, nanocellulose was blended with CTS and further compounded with anionic starch (AS) to prepare AS-CNC-CTS coating agent. And AS-CNC-CTS coating agent were used to modified one side of the surfaces of two kinds of uncoated paper using a surface-coating method to explore the impact of the interaction between the components in the coating agent, the usage amount of nanocellulose, and the effects of the properties of the backing paper on the mechanical properties (such as tear resistance, tensile strength) and barrier properties *e.g.* oil resistance and gas barrier property of the coated paper. Our results can provide a certain theoretical and data basis for the preparation of an antibacterial barrier surface-coating agent for paper and enable the exploration of a new material to replace the commonly used and nondegradable coating materials.

2 Experiment

2.1 Instruments and equipment

The instruments and equipment used were as follows: fully automatic film applicator (BEVS 181/2), scanning electron microscopy (SEM, JSM-IT500, Japan Electronics Co., Ltd., JEOL), Fourier infrared spectrometer (FT-IR, Invenior, German Bruker Company), Advance X-ray diffractometer (XRD, D8, German Bruker Company), transmission electron microscopy (TEM, JEM-2100, Japan Electronics Co., Ltd.; JEOL), paper tensile strength test machine (0.001N, Lorentzen & Wettre Shanghai Testing Equipment Co., Ltd.), computer-controlled paper tearing-strength tester (DCP-SLY1000, Sichuan Zhangjiang Paper-making Instrument Co., Ltd.), surface absorptive weight tester (YQ-Z-100, Hangzhou light industry testing instrument), oil permeability tester for paper (ZTY-100, Changchun Yueming Small Test Machine Co. Ltd.), air permeability tester for paper and paperboard (SE166, Lorentzen & Wettre Shanghai Testing Equipment Co., Ltd.), digital viscometer (NDJ-8S, Shanghai Jitai Electronic Technology Co. Ltd.), thermostatic heating agitator (DF-101S),electronic balance (FA2004B, Beijing Yinlian), and homogenizer (ESB-500X; 500 W, 28 000 rpm; Shanghai Electromechanical Equipment Co., Ltd.).

2.2 Materials and reagents

Paper samples were purchased from local supermarkets (Table 1). Carboxylated cellulose nanocrystal whisker (C-CNC) was from Guilin Qihong Technology Co., Ltd. AS (PS-268, d.s 0.03) was from Guangxi Nongken Mingyang Biochemical Group Co., Ltd. CTS ($C_{6n}H_{11n}NO_{4n}$, viscosity <200 m Pa s) was from Macklin Reagent. Glacial acetic acid (99%) was from Tianjin Kemiou Chemical Reagent Co., Ltd. Sodium hydroxide (NaOH) was from Tianjin Kemiou Chemical Reagent Co., Ltd.

2.3 Testing method

2.3.1 Preparation of AS-CNC-CTS coating. First, 1 g of CTS was placed in 100 mL of 10% acetic acid solution and stirred to dissolve. NaOH was used to adjust it to slightly acidic to prepare CTS solution (pH = 6). Then a certain amount (2, 3, or 5 g) of C-CNC was dispersed evenly into 100 mL of CTS solution to obtain CNC-CTS solution (homogenized at 28 000 rpm for 5 min). Finally, 20 g of AS was added into 100 mL of CNC-CTS solution. After stirring evenly, it was heated in a water bath, after reaching 75 °C it was stirred again for 25 min until 95 °C. Lastly, gelatinization was performed by constant-temperature (95 °C) heating before the viscosity got to 2500–2800 cp. CNC-CTS-AS coating was then obtained and denoted as 2% AS-CNC-CTS, 3% AS-CNC-CTS, and 5% AS-CNC-CTS.

2.3.2 Coating of paper. The prepared AS-CNC-CTS coating was evenly coated onto one side of the surface of kraft paper and offset paper, using fully automatic film applicator (15 μm wire bar), at the speed of 42 mm s^{-1} (once). After the coating layer was dried at the temperature of 50–60 °C, the coated paper was stored at constant temperature (23 °C ± 1 °C) and humidity (50% ± 2%) for later use.

2.3.3 Experiment for testing characterization. TEM was used to observe and analyze the morphology of C-CNC. The operating voltage was 200 kV. The C-CNC dispersion liquid with a mass fraction of 0.01% was initially prepared. Then, a piece of filter paper was taken and placed in the Petri dish. A new piece of copper mesh was placed on the filter paper with the front face upward. Next, two plastic droppers were taken, and their heads were heated with a lighter. They were stretched to become a thin needle-like tube to control the amount of dripping and facilitate operation without overturning the copper mesh. A small

Table 1 The details of paper samples in the paper

No.	Paper samples	Basis weight ($g\ m^{-2}$)	Thickness (μm)	Bekk smoothness (s)	Gloss (Gu)	Porosity (%)
1	Kraft paper	145	170	9.4	9.7	55.12[a]
2	Offset paper	83	111	27.0	11.9	47.34[a]

[a] Data originate from previous results of this research team.[8]

amount of C-CNC dispersion liquid was collected using the dropper with treated head to drip on the copper mesh (covering the whole copper mesh) carefully. Then, the Petri dish was covered and placed in a vacuum oven at 50 °C. After continuous vacuuming until the droplets were dry, the dish cover was removed and a small amount of dye (2% acetyl glaze) was dripped onto the dry copper mesh (covering the whole copper mesh). The dish was covered again and placed in darkness for 20–30 min for dyeing. Afterwards, the copper mesh was gently pressed from one side with a fine needle, and the dyeing agent was sucked from the other side with the filter paper. The obtained sample was dried at room temperature and then dried in the vacuum oven for 12 h before subjecting it to TEM analysis.

For the AS-CNC-CTS coating's antibacterial-performance test, the AS-CNC-CTS samples were sterilized on a clean workbench. The actual conditions of paper in use were simulated. After 24 h of culture, the antibacterial properties of the samples were observed.

The air permeance of paper samples before and after coating was measured with an air permeability tester for paper and paperboard in accordance with GB/T458-2008 determination of air permeance for paper and paperboard (Bentson method). The test samples were subjected to warm and wet treatment according to GB/T10739 and then cut into paper sheets 5 cm × 5 cm in size. Under the atmospheric conditions of the same warm and wet treatment, the air resistance of each paper sample before and after coating was measured. Five parallel samples were taken from each sample for measurement, and the average value was taken.

The oil resistance of paper samples before and after coating was measured with an oil permeability tester for paper in accordance with GB/T5406-2002 testing method of oil permeance for paper. After measuring the front and back of each sample three times, the average value of six values was taken.

According to GB/T455-2002 (determination of tearing resistance for paper and paperboard), the tearing resistance of paper samples before and after coating was measured using a computer-controlled paper tearing-resistance tester. Five parallel samples were taken from each paper sample in the same direction for measurement, and finally the average value was taken.

The tensile strength of paper samples was tested with paper tensile strength test machine according to GB/T12914-2018 (constant speed stretching method) (20 mm min^{-1}).

The infrared characterization of papers with dry coating were characterized by FT-IR. The scanning range was 400–4000 cm^{-1} and the resolution was 4 cm^{-1} for 64 scan times.

The X-ray diffraction were carried out on a Bruker D8 Advance X-ray diffractometer at 40 kV and 40 mA with Cu Kα radiation. The scanning speed was 0.1 s/step, with the step size of 0.02°.

The surface and cross section morphology of paper before and after coating were analyzed by SEM. The accelerating voltage was 6 kV. The paper samples were cut into paper sheets 5 mm × 5 mm in size and pasted on the conductive adhesive of the sample table. After spraied with metal, the surface of the paper was analyzed by SEM. The paper samples were cut into paper sheets 20 mm × 20 mm in size and pasted on the cross-section of the sample table. The cross section of the paper samples were analyzed by SEM after polished to 500 μm (in width) with argon ions.

3 Results and discussion

3.1 Preparation of AS-CNC-CTS coating

At present, the common nanocelluloses primarily include microfibrillated cellulose, nanofibrillated cellulose, and CNC. Among them, CNC is a kind of very small crystalline nanoparticle obtained through chemical processes, such as acid or oxidative hydrolysis. It has a negative charge and a crystallinity of more than 90%. Some studies have shown that the high crystalline region of nanocellulose can effectively hinder the penetration of gas molecules, and its blend coating has a good barrier effect on paper.[11] Accordingly, we selected C-CNC as the nanocellulose composite. Its TEM morphology is shown in Fig. 1. Image J software was used for analysis, and its diameter was 4–10 nm, length was 100–500 nm, and aspect ratio was 10–125. When the CNC content in solution was >7%, uneven dispersion and agglomeration occurred. Thus, the CNC concentration was set to 2%, 3%, and 5% in subsequent experiments.

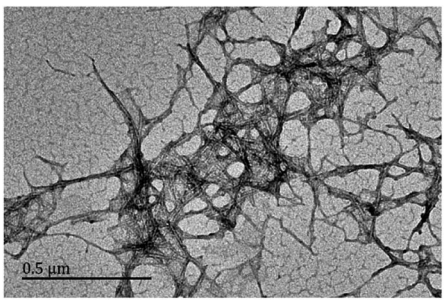

Fig. 1 TEM morphology of C-CNC used in the paper.

CTS has very poor solubility in the suspension formed by water and nanocellulose. However, it is weakly alkaline, so it has good solubility in organic acids. Accordingly, acetic acid with a concentration of 10% was selected as the solvent to prepare CTS acetic acid solution. C-CNC with carboxyl group (–COOH) was dispersed in it to make the amino group ($–NH_2$) in CTS bind with –COOH fully and form a peptide bonding, the oxhydryl (–OH) in C-CNC bind with $–NH_2$ in CTS and form a hydrogen bonding, and also the electrostatic interaction between C-CNC and CTS, thereby producing a stable CNC-CTS suspension. After adding AS for gelatinization, CTS with a positive charge after acidification ($–NH_3+$) can form strong electrostatic interaction with AS, and the hydrogen bonding between C-CNC and AS additionally, so AS-CNC-CTS became a stable system. The formed coating structure was compact without phase separation, as also confirmed by the following research results. The specific formation mechanism is shown in Fig. 2.

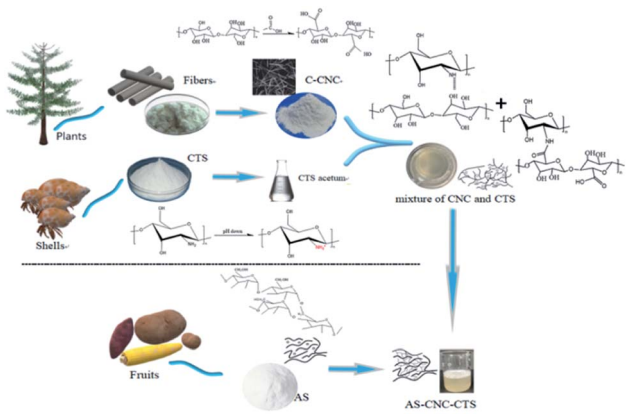

Fig. 2 Formation mechanism of AS-CNC-CTS coating.

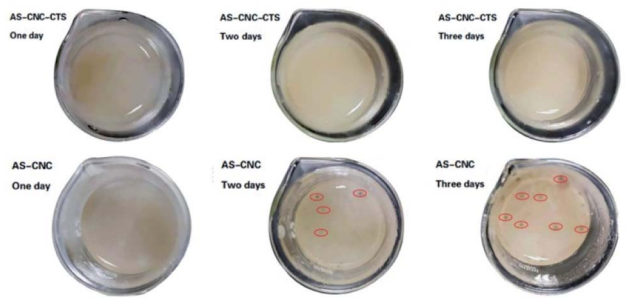

Fig. 3 Antibacterial properties of AS-CNC-CTS coating.

3.2 Properties of AS-CNC-CTS coated paper

3.2.1 Antibacterial activity. The antibacterial result of AS-CNC-CTS coating is shown in Fig. 3. Obvious mildew existed in the coating without CTS on the second day after preparation, and the mildew was more significant on the third day. The coating with CTS added had good antibacterial effect, with no mildew at the end of the observation period (60d). One of the reasons for the antibacterial properties of CTS is its positively charged amino group, which interacts with the negatively charged microbial cell membranes, resulting in the leakage of microbial proteins and other intracellular components.[26] The observation results in Fig. 3 show that the preparation process of AS-CNC-CTS coating did not destroy the antibacterial function of CTS. Therefore, in practice, AS-CNC-CTS coating can be coated onto the surface of paper to replace desiccant and mildew-proof sheet in the paper containers to solve the problem of easy mildew growth in paper containers when the humidity exceeds 80%. Additionally, if it is used as a coating agent for paper food-packaging materials, it can also protect the packaged food from mold pollution.

3.2.2 Barrier property. The barrier properties of paper against gas are generally characterized by air permeance. If the air permeance is lower, its air barrier effect is better. Conversely, if the air permeance is high, the barrier effect is poor. Eqn (1) is the calculation of air permeance (P).

$$P = 0.0113q \quad (1)$$

where P refers to the air permeance under 1.47 kPa standard pressure difference, in μm (Pa s^{-1}); and q refers to the volume of air passing through the testing surface of the sample per minute, in mL min^{-1}.

The air permeance of the paper samples before and after coated is shown in Table 2. Under the same laboratory conditions, the mean deviation of the measurement results of two test pieces from the same sample by the same operator was within 10%.

Table 2 shows that the air permeance of kraft paper and offset paper before coated was very high, *i.e.*, 12.2000 (μm (Pa s^{-1})) and 10.0200 (μm (Pa s^{-1})), respectively. Moreover, the air permeance of kraft paper was higher than that of offset paper. This finding was due to the porous structure of the paper itself. It significantly decreased after coated, indicating that a dense film formed after coated AS-CNC-CTS onto the surface of paper, thereby significantly improving the air-barrier property of paper.

Generally, many methods can characterize the oil resistance of paper, oil absorbance is used in this paper. According to GB/T5406-2002, the calculation equation of oil absorbance is shown as eqn (2).

Table 2 Air permeance (μm (Pa s^{-1})) of the paper samples

No.	Paper sample	Uncoated	2% AS-CNC-CTS	3% AS-CNC-CTS	5% AS-CNC-CTS
1	Kraft paper	12.2000	0.0250	0.0099	0.0069
2	Offset paper	10.0200	0.0145	0.0098	0.0074

Table 3 Oil absorbance (g m^{-2}) of paper samples in this work

No.	Paper sample	Uncoated	2% AS-CNC-CTS	3% AS-CNC-CTS	5% AS-CNC-CTS
1	Kraft paper	446.54	11.73	8.73	7.09
2	Offset paper	413.72	5.62	2.42	1.81

$$p = \frac{m_2 - m_1}{0.01} \quad (2)$$

where p refers to oil absorbance, in g m^{-2}; m_1 refers to the weight of filter paper before oil absorption, in g; and m_2 refers to the weight of filter paper after oil absorption, in g. The measured data were substituted into eqn (2) to calculate the oil absorbance of the paper samples before and after coated, as shown in Table 3.

According to the data in Table 3, similar to the air-barrier property, the oil resistance of all paper samples greatly increased after coated, and the effective of oil resistance are shown in Fig. 4. This finding was consistent with existing research results.[28,29]

According to Tables 2 and 3, with increased C-CNC content in the coating, the air-barrier property and oil resistance of coated paper gradually increased. This result is consistent with the good barrier property of the crystal part of C-CNC which mentioned in the literature.[25] Furthermore, neither oxygen (air) nor oil can interact with the hydrogen bond structure of nanocellulose, CTS and AS, also directly improving the barrier of coated paper to gas and oil. Among them, when C-CNC increased from 2% to 3%, barrier property significantly improved. However, when it increased from 3% to 5%, barrier property insignificantly improved. The reason may be that with increased C-CNC content, the crystal area enlarged, and the bonding interaction between CNC and AS, CNC and CTS, CNC and paper fibers were enhanced. Additionally, the binding force between the fibers inside the paper enlarged, and the air barrier and oil resistance were enhanced. However, when the content continued to increase, CNC gradually aggregated, which weakened the bonding interaction and the binding force between the fibers inside the paper. Consequently, the barrier enhancement effect was insignificant. Comprehensively considering the effects and costs of raw materials, 3% AS-CNC-CTS was selected in subsequent experiments.

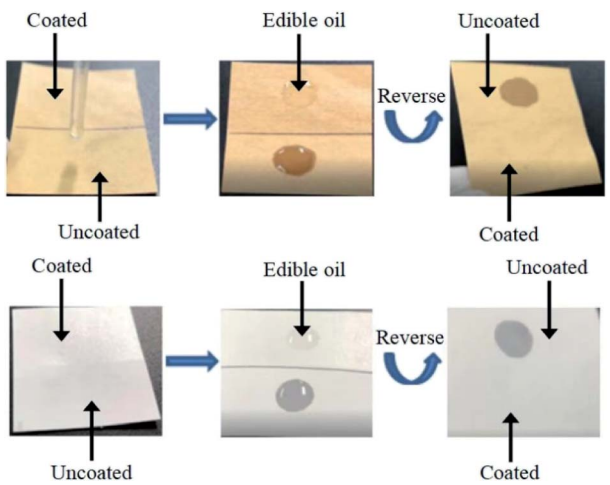

Fig. 4 Effective of oil resistance of kraft paper (5 cm × 5 cm) and offset paper (5 cm × 5 cm) before and after coated.

Table 4 Tearing resistance and tensile strength of paper samples before and after coated

		Horizontal vertical			
No.	Paper sample	Tearing resistance (mN)		Tensile strength (N m^{-1})	
1	Uncoated kraft paper	1322.5	578.6	4140.0	8746.7
2	Coated kraft paper	1471.8	689.3	4586.7	8993.3
3	Uncoated offset paper	386.7	196.2	1873.3	4666.7
4	Coated offset paper	389.5	200.3	1973.3	4701.3

3.2.3 Tearing resistance and tensile strength. The tearing resistance and tensile strength of paper is defined as the force required to tear a certain length of paper and the maximum tension that paper or cardboard can withstand before breaking respectively. Both of them are the most common indicators to characterize the mechanical properties of paper. The tearing resistance and tensile strength of kraft paper and offset paper before and after coated with 3% AS-CNC-CTS was measured. Results are shown in Table 4.

From Table 4, we find that the tearing resistance and tensile strength of coated kraft paper significantly improved, increasing by 19.1% (vertical) and 10.9% (horizontal) respectively, and the change for offset paper is smaller. The reason may be that kraft paper had high porosity, and more coatings penetrated its pore structure, which enhanced the adhesion between fibers inside the paper and thus improved the tear resistance and tensile strength. Conversely, the porosity of offset paper was relatively low, and the coating is primarily attached to the surface, forming a uniform coating on the surface to fill the pores formed between the surface fibers. However, it had little effect on the interaction between the internal fibers.

3.3 Characterization of AS-CNC-CTS coated paper

3.3.1 FT-IR characterization. In terms of the blends of two or more substances, their properties depend on the properties, morphology, and phase interface of various components, especially the compatibility of components, which is an important basis to judge the blending effect. The amino group in the molecular structure of CTS can have hydrogen-bond interaction with the hydroxyl group of nanocellulose. The

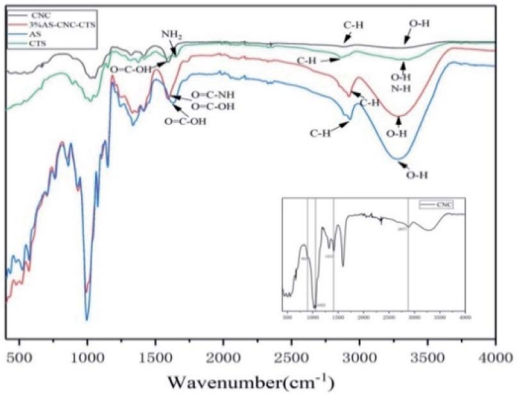

Fig. 5 FT-IR spectra of carboxylated cellulose nanocrystal whisker (C-CNC), chitosan (CTS), anionic starch (AS), and 3% AS-CNC-CTS coated layer.

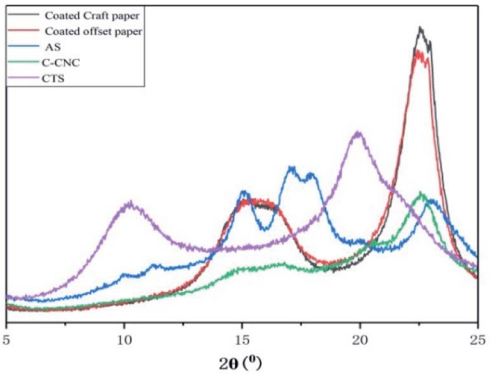

Fig. 6 XRD of carboxylated cellulose nanocrystal whisker (C-CNC), chitosan (CTS), anionic starch (AS), and 3% AS-CNC-CTS coated paper.

amino group can also acylate with the carboxyl group of carboxylated nanocellulose, which is conducive to improving the compatibility between them. Infrared spectroscopy is one of the most effective means to study bonding interaction. Accordingly, we studied the interaction between the components in 3% AS-CNC-CTS coating film by using infrared spectroscopy. Fig. 5 shows the infrared spectra of C-CNC, CTS, AS, and 3% AS-CNC-CTS coating film.

In the infrared spectrum of AS, a –OH stretching vibration absorption peak appeared at 3283 cm^{-1}, and a O=C–OH vibration absorption peak at 1630 cm^{-1}. In the infrared spectrum of C-CNC, the strong absorption peak at 3300 cm^{-1} was attributed to the stretching vibration peak of hydroxyl (–OH) in cellulose molecules. The absorption peaks at 2877 and 1413 cm^{-1} were the stretching and bending vibration peaks of methylene ($–CH_2–$) respectively, the former was the crystallization reference peak of cellulose, whereas the latter was its crystallization peak of cellulose. The absorption peak at 1590 cm^{-1} was the O=C–OH vibration absorption peak, that at 1055 cm^{-1} was cellulose C6 bit C–O stretching vibration, and that near 895 cm^{-1} was attributed to the stretching vibration of C1–O–C4, which was the characteristic absorption peak of β-D-glucopyranose.[30] In the infrared spectrum of CTS, the absorption peak near 3300 cm^{-1} was the stretching vibration multiple absorption peaks of hydroxyl (–OH) and amino (–NH) in CTS molecules, that at 2863 cm^{-1} was the C–H stretching vibration, and that at 1588 cm^{-1} was the acylamino vibration absorption peak.[31] In the infrared spectrum of 3% AS-CNC-CTS coating layer, the absorption peak at 2920 cm^{-1} was the C–H stretching vibration, indicating that the crystallization reference peak of nanocellulose still existed. Vibration peaks of O=C–NH and O=C–OH were found at 1590 cm^{-1}, indicating that –COOH in CNC (and AS) bonded with $–NH_2$ in CTS. Dipole moment greatly changed owing to the bonding interaction, so the intensity of its absorption peak increased. Moreover, the bonding interaction between –COOH and $–NH_2$ led to decreased force constant of O=C–OH chemical bond in AS, so its absorption frequency moved toward the direction with low wavenumber. The same covalent bond was also found in the literature.[32]

3.3.2 XRD characterization. Fig. 6 shows the XRD pattern of the coated paper and various components of AS-CNC-CTS coating. The patterns revealed diffraction peaks of CTS at 10.7° and 19.8°, belonging to the (020) and (100) crystallographic planes, respectively.[33] Diffraction peaks of C-CNC were found at 14.8°, 16.3°, and 22.6°, which indicated the typical cellulose type I structure.[30,31] However, the crystal structure of AS-CNC-CTS coating on paper surface differed from those of C-CNC and CTS. Fig. 6 also shows that the diffraction peaks of the XRD patterns are the basically same shape for the different coated paper. A wide diffraction peak was found at $2\theta = 22.5°$, which may be due to the superposition of diffraction peaks at 22.6° (C-CNC) and 19.8° (CTS). This diffraction peak was very strong, indicating a high crystallinity. The reason was that the covalent bond formed between CTS and C-CNC enhanced the binding force between molecular chains, leading to the coating's crystallization during drying and curing.

3.3.3 SEM characterization. To further study the micromorphology of 3% AS-CNC-CTS coating on the surface of the paper sample, the penetration extent of the coating to the pores between the fibers, the thickness of the coating, the surface and cross section of the paper sample before and after coated were analyzed by SEM. Results are shown in Fig. 7.

By analyzing the surface and cross section views of the coated paper samples [Fig. 7(b, c, e and f)], we found that regardless of the morphology of the base paper itself, the coating formed a dense film on the paper surface, which evenly attached to the paper surface and filled all pores on the surface. Thus, the surface was flat and smooth, indicating good compatibility between various components in the coating. This finding was consistent with FT-IR results. The cross section views of coated paper [Fig. 7(c) and (f)] revealed that the coating penetrated to the pores between fibers, forming a continuous-phase interface. No obvious gap existed between the paper fibers and coating, again indicated the good compatibility among various components in the coating.

Fig. 7(c) and (f) also show that the thickness of continuous phase of the coating in the pores of fibers is different due to the irregular pore structures of the paper. The difference between maximum thickness and the minimum thickness of the coating

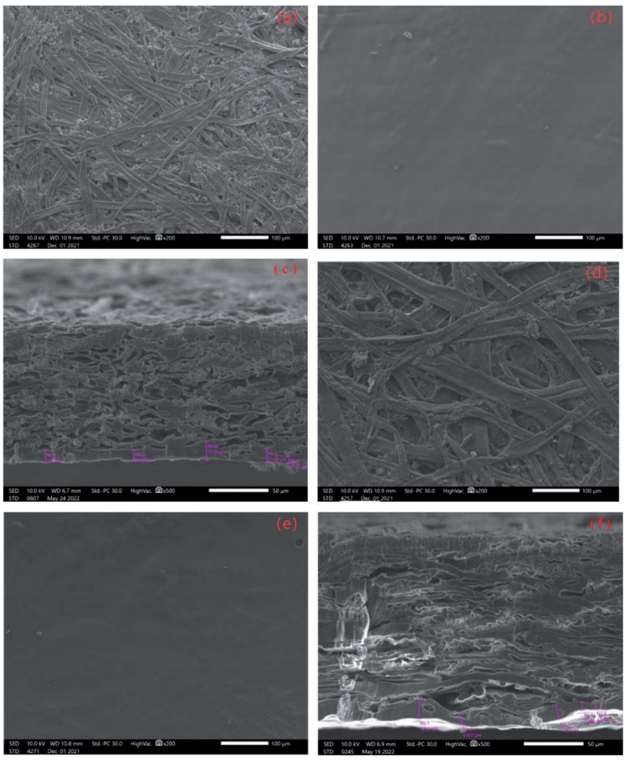

Fig. 7 (a) Uncoated offset paper (front view), (b) coated offset paper (front view), (c) coated offset paper (side view), (d) uncoated kraft paper (front view), (e) coated kraft paper (front view), and (f) coated kraft paper (side view).

film in the pores of kraft paper was 11.730 μm, whereas that was just 9.633 μm for offset paper. This finding may be due to the lower surface smoothness and higher porosity of kraft paper, higher penetration rate of the coating in the pores formed by the intersection of fibers. The biggest penetration depth of the coating into the pores of kraft paper fiber was larger than the offset paper, so it played a greater role in enhancing the adhesion between fibers. This finding was also consistent with the experimental results of tearing resistance and tensile strength previously mentioned.

4 Conclusions

A high-speed homogenizer was used to disperse C-CNC into CTS acidic solution under high-speed stirring so that the carboxyl group of C-CNC formed a strong peptide bonding interaction with the amino group of CTS, the hydrogen bonding between C-CNC and CTS. Then, it was gelatinized with AS to form a stable AS-CNC-CTS coating system. The coating had good compatibility while retaining some crystal regions of CNC and the antibacterial properties of CTS.

AS-CNC-CTS coating can well attach to the paper surface, forming a dense coating film. While improving tearing resistance and tensile strength of paper, it conferred the paper with antibacterial properties and enhanced the air barrier and oil resistance of paper. This study can provide a method of preparing a paper surface-coating agent with excellent comprehensive and antibacterial properties. This surface-coating agent is expected to replace the commonly used nondegradable coating materials for the dry and fatty food packaging materials.

Conflicts of interest

We declare that we do not have any commercial or associative interest that represents a conflict of interest in connection with the work submitted.

Acknowledgements

This work was supported by Guangdong Basic and Applied Basic Research Foundation (2019A1515110667) and Dongguan City Social Development Science and Technology Project (2022, Key Projects).

References

1 H. Y. Cui, D. Surendhiran, C. Z. Li and L. Lin, *Food Packag. Shelf Life*, 2020, **24**, 100511.
2 J. L. Xu, X. P. Zhong, Y. M. Zhu, X. Y. Yang, W. H. Wang, Y. Liu, F. Li, Q. Liu, L. J. Li, X. F. Liu, L. Zou and H. Chen, *Plast. Ind.*, 2017, **3**, 1–44.
3 R. G. Newell, Y. F. Qian and D. Raimi, *Global Energy Outlook 2015, NBER Working Paper Series*, National Bureau of Economic Research, 2016.
4 S. Q. Cui, J. Borgemenke, Y. S. Qin, Z. Liu and Y. B. Li, *Adv. Bioenergy*, 2019, 15–50.
5 B. Bideau, E. Loranger and C. Daneault, *Prog. Org. Coat.*, 2018, **123**, 128–133.
6 H. Terhi, V.-N. Mika, H. Ali and K. Maarit, *Thin Solid Films*, 2010, **518**, 5463–5466.
7 K. Khaoula, A. T. Elmira and D. Stephane, *Compr. Rev. Food Sci. Food Saf.*, 2010, **9**, 82–91.
8 M. G. Xue, H. Q. Chen, H. Li, H. Wei and W. Li, *China Pulp Pap.*, 2020, **39**, 50–54.
9 X. L. Wu and Y. Jing, *Trans. China Pulp Pap.*, 2016, **31**, 1–6.
10 V. Kumar, E. Kenttä, P. Andersson and U. Forsström, *Coatings*, 2020, **10**, 1108.
11 P. Tyagi, M. A. Hubbe, L. Lucia and L. Pal, *Cellulose*, 2018, **25**, 3377–3391.
12 Y. S. Liu, *Study on the Barrier Coating of Paper and Its Barrier Performance*, 2012.
13 S. H. Zhang, R. F. Fu, L. Q. Dong, Y. C. Gu and S. Chen, *China Pulp Pap.*, 2017, **36**, 67–74.
14 G. Fotie, S. Limbo and L. Piergiovanni, *Nanomaterials*, 2020, **10**, 1–26.
15 D. Alain, *Pap. Biomater.*, 2020, **5**, 1–13.
16 R. Liu, P. Lu, M. Wu and C. X. Huang, *Packag. Eng.*, 2019, **40**, 51–59.
17 Z. H. Li. *Preparation and Application of Chitosan based Biomass Antibacterial Material*, 2016, pp. 3–11.
18 S. Park and Y. Y. Zhao, *J. Agric. Food Chem.*, 2004, **52**, 1933–1939.

19 N. E. Suyatma, L. Tighzert, A. Copinet and V. Coma, *J. Agric. Food Chem.*, 2005, **53**, 3950–3957.
20 T. Wu, S. Zivanovic, F. Ann Draughon, W. S. Conway and C. E. Sams, *J. Agric. Food Chem.*, 2005, **53**, 3888–3894.
21 K. N. Matsui, F. D. S. Larotonda, S. S. Paes, D. B. Luiz, A. T. N. Pires and J. B. Laurindo, *Carbohydr. Polym.*, 2004, **55**, 237–243.
22 G. Davis and J. H. Song, *Ind. Crops Prod.*, 2006, **23**, 147–161.
23 J. J. Kester and O. Fennema, *J. Am. Oil Chem. Soc.*, 1989, **66**, 1139–1146.
24 W. L. Dong, *Packag. Eng.*, 2009, **30**, 117–120.
25 L. Alves, E. Ferraz and G. Jaf, *Adv. Colloid Interface Sci.*, 2019, **272**, 101994.
26 P. K. A. Dutta, J. B. Dutta and V. S. B. Tripathi, *J. Sci. Ind. Res. India.*, 2004, **63**, 20–31.
27 I. Aranaz, M. Mengibar, R. Harris, I. Panos, B. Miralles, N. Acosta, G. Galed and A. Heras, *Curr. Chem. Biol.*, 2009, **3**, 203–230.
28 M. Österberg, J. Vartiainen, J. Lucenius, U. Hippi, J. Seppälä, R. Serimaa and J. Laine, *ACS Appl. Mater. Interfaces*, 2013, **5**, 4640–4647.
29 V. A. Kisonen, K. B. Prakobna, C. A. B. Xu, A. C. Salminen, K. S. D. Mikkonen, D. E. Valtakari, P. F. Eklund, J. C. Seppälä, M. D. Tenkanen and S. A. Willför, *J. Mater. Sci.*, 2015, **50**, 3189–3199.
30 Y. C. Wang, H. L. He, Q. Wang, S. S. Liu, Y. S. Mu and C. X. Han, *China Pulp Pap.*, 2020, **39**, 18–25.
31 W. Y. Bao, C. Xu, F. Song, X. L. Wang and Y. Z. Wang, *Acta Polym. Sin.*, 2015, **1**, 49–56.
32 R. M. Chen, C. Zhao, Z. P. Chen, X. Y. Shi, H. X. Zhu, Q. Bu, L. Wang, C. F. Wang and H. He, *Biomaterials*, 2022, **281**, 121330.
33 F. Tian, Y. Liu, K. Hu and B. Y. Zhao, *J. Mater. Sci.*, 2003, **38**, 4709–4712.